

Theory for the three-dimensional Mercedes-Benz model of water

Alan Bizjak,¹ Tomaz Urbic,^{1,a)} Vojko Vlachy,¹ and Ken A. Dill²

¹*Faculty of Chemistry and Chemical Technology, University of Ljubljana, Aškerčeva 5, 1000 Ljubljana, Slovenia*

²*Department of Pharmaceutical Chemistry, University of California, San Francisco, California 94143-1204, USA*

(Received 23 April 2009; accepted 16 October 2009; published online 16 November 2009)

The two-dimensional Mercedes-Benz (MB) model of water has been widely studied, both by Monte Carlo simulations and by integral equation methods. Here, we study the three-dimensional (3D) MB model. We treat water as spheres that interact through Lennard-Jones potentials and through a tetrahedral Gaussian hydrogen bonding function. As the “right answer,” we perform isothermal-isobaric Monte Carlo simulations on the 3D MB model for different pressures and temperatures. The purpose of this work is to develop and test Wertheim’s Ornstein–Zernike integral equation and thermodynamic perturbation theories. The two analytical approaches are orders of magnitude more efficient than the Monte Carlo simulations. The ultimate goal is to find statistical mechanical theories that can efficiently predict the properties of orientationally complex molecules, such as water. Also, here, the 3D MB model simply serves as a useful workbench for testing such analytical approaches. For hot water, the analytical theories give accurate agreement with the computer simulations. For cold water, the agreement is not as good. Nevertheless, these approaches are qualitatively consistent with energies, volumes, heat capacities, compressibilities, and thermal expansion coefficients versus temperature and pressure. Such analytical approaches offer a promising route to a better understanding of water and also the aqueous solvation. © 2009 American Institute of Physics. [doi:10.1063/1.3259970]

I. INTRODUCTION

A goal of liquid-state theory has been to develop a statistical mechanical theory of water. There is a long history of modeling water^{1–5} and both its pure state and in mixture with various solutes.^{6–11} In general we can divide solvation models into two classes: explicit models, which treat water on equal level as solute particles, and implicit ones, where water is characterized merely by its dielectric constant. Explicit models, such as transferable intermolecular potential (TIP),^{12–14} simple point charge (SPC) (Ref. 15) and others, are presently computationally too expensive to obtain the concentration dependence of thermodynamic quantities for complex biological systems. On the other hand implicit models, coupled with the Poisson–Boltzmann approach, often miss much of the physics of solvation and may lead to erroneous predictions. There are also a couple of theories with treatments of water’s unusual density behavior using double-well spherically symmetric potentials^{16,17}

To improve solvation models, we need to better understand pure water. Ideally, it would be preferable to have a model of water that is both computationally fast and physically sound. Several simple two-dimensional (2D) and three (3D) models have been proposed in Refs. 9 and 18–25. These models do not require extensive computing yet they yield reasonably good agreement with experimental data on real water. One such model, in analogy with its 2D predecessor^{21,26} called 3D Mercedes-Benz model (3D MB),

originally proposed by Ben-Naim in 1974,²⁷ has recently been examined by computer simulations.²⁵ According to the 3D MB model, each water molecule is a Lennard-Jones (LJ) sphere with four arms, oriented tetrahedrally to mimic hydrogen bonding. This model has been studied by Monte Carlo (MC) computer simulations. However, there would be benefit to having analytical theories, such as integral equations or thermodynamic perturbation theories. In principle, they are computationally much more efficient, and they express more directly physical insights. In several contributions from our group, Wertheim’s Ornstein–Zernike (WOZ) integral equation theory²⁸ and thermodynamic perturbation approach^{28,29} were applied to simple models of water and aqueous solutions.^{22,30–33} While traditional OZ approaches have not been very good for systems with highly directional forces and strong association, such as water, the WOZ approach promises to be much more successful. The integral equation approach proposed by Wertheim is free of the convergence problems that are often associated with the regular OZ theory in the hypernetted-chain approximation.

Here, our goal is to test the thermodynamic perturbation theory (TPT) of Wertheim^{28,29} and the corresponding WOZ integral equation approach²⁸ against MC simulations of the 3D MB model of Ref. 25.

While our paper was in review, Dias *et al.*³⁴ published a modified version of the 3D MB model, with different parameters to better reproduce the solid phase (ice) and the pair distribution function. While doing this they have introduced several new parameters (5). In addition their interaction potential depends on local environment.

^{a)}Electronic addresses: tomaz.urbic@fkkt.uni-lj.si and tomaz@urbic.com.

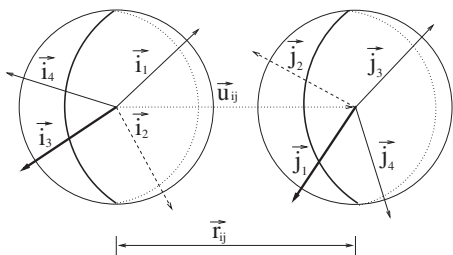


FIG. 1. Two molecules of 3D MB water (i and j), separated by the distance r_{ij} . Each molecule has four bonding vectors denoted by \vec{i}_k (or \vec{j}_l); $k, l=1, 2, 3$, and 4.

II. MODELING WATER

In this model, each water molecule is represented as a LJ particle having four arms oriented tetrahedrally. The angle between neighboring arms in a molecule is 109.4° (see Fig. 1). Figure 1 shows the molecules with their bonding arms oriented in space. The intermolecular axis is denoted by \vec{u}_{ij} . A hydrogen bond (HB) between two water molecules is formed when the arm of one molecule is aligned with the arm of an adjacent neighboring water molecule.

The interaction potential between two water molecules is a sum of the LJ potential and the HB term,

$$U(\vec{X}_i, \vec{X}_j) = U_{\text{LJ}}(r_{ij}) + U_{\text{HB}}(\vec{X}_i, \vec{X}_j), \quad (1)$$

where r_{ij} is the distance between centers of particles i and j , and \vec{X}_i denotes the vector representing the coordinates and the orientation of the i th particle. The LJ part of the potential is

$$U_{\text{LJ}}(r_{ij}) = 4\epsilon_{\text{LJ}} \left[\left(\frac{\sigma_{\text{LJ}}}{r_{ij}} \right)^{12} - \left(\frac{\sigma_{\text{LJ}}}{r_{ij}} \right)^6 \right], \quad (2)$$

where ϵ_{LJ} and σ_{LJ} are the well depth and the contact parameter, respectively. The hydrogen bonding part of the interaction potential is

$$U_{\text{HB}}(\vec{X}_i, \vec{X}_j) = \sum_{k,l=1}^4 U_{\text{HB}}^{kl}(r_{ij}, \vec{\Omega}_i, \vec{\Omega}_j), \quad (3)$$

where $\vec{\Omega}_i$ is the orientational vector of i th molecule and U_{HB}^{kl} describes the interaction between two HB arms of different molecules,

$$U_{\text{HB}}^{kl}(r_{ij}, \vec{\Omega}_i, \vec{\Omega}_j) = \epsilon_{\text{HB}} G(r_{ij} - r_{\text{HB}}) G(\vec{i}_k \vec{u}_{ij} - 1) G(\vec{j}_l \vec{u}_{ij} + 1). \quad (4)$$

\vec{u}_{ij} is the unit vector along \vec{r}_{ij} and \vec{i}_k is the unit vector representing the k th arm of the i th particle. In Eq. (4) $G(x)$ is an unnormalized Gaussian function, defined by

$$G(x) = e^{-x^2/2\sigma^2}. \quad (5)$$

The strongest HB occurs when an arm of one particle is colinear with the arm of another particle pointed toward each other. The model does not make a distinction between HB donors and acceptors.

Apart from the dimensionality, we want to keep the 3D MB model as similar as possible to the original 2D MB model. Hence, the parameters of our 3D model are the same

as used in the 2D MB model calculations, with an exception of the depth of the LJ potential well ϵ_{LJ} . This change was made to maintain same ratio between strength of the LJ and HB potentials due to the different geometries. In total there are five parameters describing the water molecule. Here, we use the values: $\epsilon_{\text{HB}} = -1$, and $\epsilon_{\text{LJ}} = \frac{1}{35} |\epsilon_{\text{HB}}|$; the width of the Gaussian function $\sigma = 0.085$ was chosen to be small enough that a direct HB is more favorable than a bifurcated one. The contact LJ distance σ_{LJ} is $0.7r_{\text{HB}}$, where $r_{\text{HB}} = 1$. These model parameters were not chosen or optimized to compare with experiments, and can undoubtedly be improved for those purposes. Our goal here is simply to take a 3D waterlike model having waterlike properties and test how well the statistical mechanical Wertheim theories agree with computer simulations. All thermodynamic quantities will be reported in reduced units normalized to the strength of the optimal HB: $T^* = k_B T / |\epsilon_{\text{HB}}|$, $U^{ex*} = U^{ex} / |\epsilon_{\text{HB}}|$, $V^* = V / r_{\text{HB}}^3$, and $P^* = P r_{\text{HB}}^3 / |\epsilon_{\text{HB}}|$. Similarly, all the distances are scaled by the length of the HB separation ($r_{\text{HB}} = 1$).

III. COMPUTER SIMULATIONS

Our MC simulations were performed in the isothermal-isobaric (NPT) ensemble. In simulation (for details see also Ref. 25) periodic boundary conditions and the minimum image convention were used to mimic an infinite system of particles. Starting configurations were selected randomly except for temperatures below $T^* = 0.2$ where we also started from a diamond crystal lattice (cubic ice structure). The diamond crystal lattice was formed by the water molecules consisting of two interpenetrating face-centered cubic Bravais lattices, displaced along the body diagonal of the cubic cell by one quarter the length of the diagonal. Euler angles for first fcc lattice were set to $(\pi/2, \pi/2, \pi/2)$ and for the second fcc lattice $(\pi/2, \pi/2, 0)$. If the results (fluid density, energy) were found to be independent of the starting configuration we take this as an indication of the liquid phase. According to the simulations the liquid water exists above $T^* \approx 0.13$ at $P^* = 0.12$ and $T^* \approx 0.12$ for $P^* = 0.19$.

For equilibration we used 10^5 moves per particle, which was more than enough to stabilize reduced molar volume and reduced internal energy. Statistics were sampled over the next 10^6 moves per particle. To estimate numerical uncertainties every simulation was divided into ten independent blocks. All simulations were performed with $N = 500$ water molecules, with the exception when we started from crystal lattice. There we used 512 particles. To hold the pressure constant, an attempt was made to scale the dimensions of the box after every pass (one pass was equal to N attempted moves). Mechanical properties, such as reduced excess internal energy, U^{ex*} , and the reduced molar volume, V_n^* , are calculated as the statistical averages of these quantities.³⁵ The reduced heat capacity C_p^* , reduced isothermal compressibility κ^* , and the reduced thermal expansion coefficient α^* are computed using fluctuation formulas,²¹ and therefore are associated with much larger uncertainties than simple averages such as molar volume. The relevant formulas are given below:

$$C_P^* = \frac{C_P}{k_B} = \frac{\langle H^{*2} \rangle - \langle H^* \rangle^2}{NT^{*2}}, \quad (6)$$

$$\kappa^* = \frac{\langle V^{*2} \rangle - \langle V^* \rangle^2}{T^* \langle V^* \rangle}, \quad (7)$$

$$\alpha^* = \frac{\langle V^* H^* \rangle - \langle V^* \rangle \langle H^* \rangle}{T^{*2} \langle V^* \rangle}. \quad (8)$$

The calculations were performed in a range of the reduced temperatures between $T^*=0.10$ and $T^*=0.5$, but the results presented here apply to the liquid phase only. In order to discuss the effect of pressure on water properties, we present a set of new results obtained for $P^*=0.19$, while the simulations for $P^*=0.12$, published before,²⁵ were refined and extended to longer MC runs.

IV. ANALYTICAL APPROACHES

In this section we apply the first-order thermodynamic perturbation^{28,29,18} theory and the integral equation approach^{28,36,37} to the 3D MB model of water described in Sec. II.

A. Thermodynamic perturbation theory

The main quantity in the TPT (Ref. 28) is the Helmholtz free energy, A , of the system, which is in our case sum of the LJ and HB contributions,

$$\frac{A}{Nk_B T} = \frac{A_{LJ}}{Nk_B T} + \frac{A_{HB}}{Nk_B T}. \quad (9)$$

N denotes the number of particles, T is the temperature, and k_B is the Boltzmann constant. The LJ contribution, A_{LJ} , is calculated using the Barker–Henderson approximation³⁸ with the hard-sphere fluid as a reference system,

$$\frac{A_{LJ}}{Nk_B T} = \frac{A_{HS}}{Nk_B T} + \frac{2\pi\rho}{k_B T} \int_{\sigma_{LJ}}^{\infty} g_{HS}(r, \eta) U_{LJ}(r) r^2 dr. \quad (10)$$

Here A_{HS} is the hard-sphere contribution to the Helmholtz free energy, ρ is the number density of particles, and η the packing fraction defined by

$$\eta = \frac{\rho\pi d^3}{6}. \quad (11)$$

The diameter d of hard-spheres, composing the reference system, is obtained from the integral,

$$d = \int_0^{\sigma_{LJ}} \left[1 - \exp\left(-\frac{U_{LJ}}{k_B T}\right) \right] dr. \quad (12)$$

To calculate the hard-sphere term of the Helmholtz free energy, the Carnahan–Starling expression³⁹ was integrated to obtain the equation of state,

$$\frac{A_{HS}}{Nk_B T} = \int_0^\eta \frac{Z-1}{\eta} d\eta, \quad (13)$$

where Z is

$$Z = \frac{1 + \eta + \eta^2 - \eta^3}{(1 - \eta)^3}. \quad (14)$$

Finally the pair distribution function of the hard-sphere system, $g_{HS}(r, \eta)$, was approximated by the expression of Gonzales *et al.*⁴⁰

For the hydrogen bonding term of the Helmholtz free energy,⁴¹ A_{HB} , we use the expression originally derived by Wertheim,²⁸

$$\frac{A_{HB}}{Nk_B T} = 4 \left(\ln x_i - \frac{x_i}{2} + \frac{1}{2} \right). \quad (15)$$

In this equation x_i is the fraction of molecules not bonded at arm i , where i stands for A, B, C, or D. The fraction x_i is calculated with the help of the mass-action law in the form

$$x_i = \frac{1}{1 + 4\rho x_i \Delta}. \quad (16)$$

Finally Δ is defined by^{28,41}

$$\Delta = 4\pi \int g_{LJ}(r) \langle f_{HB} \rangle r^2 dr, \quad (17)$$

where $\langle f_{HB} \rangle$ is an orientationally averaged Mayer function for the hydrogen bonding potential of one site. The pair distribution function for the LJ system of particles, $g_{LJ}(r)$, is obtained by solving the OZ integral equation in the Percus–Yevick approximation.³⁸ Once the Helmholtz free energy is known, other thermodynamic quantities can easily be calculated.³⁸

B. Integral equation theory

The TPT does not give information about mutual correlations of fluid particles. In order to compute quantities of that type, it is necessary to use the integral equation theory.²⁸

The latter is usually in better agreement with computer simulations than the perturbation theory. In the present work we use the orientationally averaged version of the WOZ integral equation in the polymer Percus–Yevick (PPY) closure.^{28,36,37}

In the orientationally averaged version of the WOZ integral equation, the positions of bonding arms of molecule are not fixed relative to each other, so the intramolecular angles between the arms can assume random values. Clearly, this is a substantial simplifying assumption that is not made within the MC simulations.²⁵ A similar approximation is built into the TPT, where the reference system with spherical symmetry is used.⁴¹

The WOZ equation can be written in form

$$\hat{\mathbf{h}}(k) = \hat{\mathbf{c}}(k) + \hat{\mathbf{c}}(k)\boldsymbol{\rho}\hat{\mathbf{h}}(k), \quad (18)$$

where $\hat{\mathbf{h}}(k)$ and $\hat{\mathbf{c}}(k)$ are the matrices whose elements are the Fourier transforms of the partial correlation functions $h_{ij}(r)$ and $c_{ij}(r)$, respectively. Furthermore, $\boldsymbol{\rho}$ is the matrix containing the partial densities; see Eq. (20) below. The indices i and j denote the bonding states of the corresponding particles and assume the values 0, 1, 2, 3, and 4. In this study we restrict ourselves to the so-called “ideal network” approxi-

mation, which neglects all the partial correlation functions with at least one of the indices $i, j \geq 2$.²² By taking into account the equivalence of the bonding arms we have

$$\hat{w}(k) = \begin{pmatrix} \hat{w}_{00}(k) & \hat{w}_{01}(k) \\ \hat{w}_{10}(k) & \hat{w}_{11}(k) \end{pmatrix}, \quad (19)$$

where w stands for either the h or c correlation function, and ρ is the matrix containing the partial densities,

$$\rho = \begin{pmatrix} \rho & 4\rho \\ 4\rho & 12\rho \end{pmatrix}. \quad (20)$$

In order to solve the Eq. (18) an appropriate additional (closure) relation between h and c correlation functions is needed. In present study the PPY closure²⁸ is used,

$$c_{ij}(r) = f_{Lj}(r)y_{ij}(r) + \delta_{i1}\delta_{j1}\langle f_{HB}(r) \rangle y_{00}x_i^2 e_{Lj}(r), \quad (21)$$

where $y_{ij}(r) = t_{ij}(r) + \delta_{0i}\delta_{0j}$ and $t_{ij}(r) = h_{ij}(r) - c_{ij}(r)$, x_i is the fraction of particles not bonded at one particular arm i , $f_{Lj}(r) = e_{Lj}(r) - 1$ and

$$e_{Lj} = \exp\left(-\frac{U_{Lj}}{k_B T}\right).$$

As before $\langle f_{HB}(r) \rangle$ is the orientationally averaged Mayer function for the hydrogen bonding potential and x_i follows from Eq. (16). The total pair distribution function $g(r)$ is obtained by summing up the partial distribution functions,

$$g(r) = g_{00}(r) + 4g_{01}(r) + 4g_{10}(r) + 16g_{11}(r), \quad (22)$$

where $g_{ij}(r) = h_{ij}(r) + \delta_{i0}\delta_{j0}$.

Once partial pair distribution functions are known the thermodynamic properties can be calculated. For example, the excess internal energy, U^{ex} , is calculated from the expression⁴²

$$\frac{U^{ex}}{Nk_B T} = \frac{2\pi\rho}{k_B T} \left[\int g(r)U_{Lj}r^2 dr + 16x_i^2 \int g_{00}(r) \times \langle U_{HB} f_{HB} \rangle r^2 dr \right], \quad (23)$$

where $u_{HB} = U_{HB}^{kl}$ for any pair k and l . The pressure can be obtained via the virial equation,⁴³

$$P = \rho k_B T - \frac{2\pi}{3} \rho^2 \left[\int r^3 g(r) \frac{dU_{Lj}}{dr} dr + 16x_i^2 \int g_{00}(r) \times \left\langle \frac{dU_{HB}}{dr} f_{HB} \right\rangle r^3 dr \right]. \quad (24)$$

Other thermodynamic quantities, such as reduced isothermal compressibility, κ_T^* , reduced thermal expansion coefficient, α^* , and reduced heat capacity at constant pressure, C_p^* , are obtained using the definitions, where C_v^* is the reduced heat capacity at constant volume,

$$(\kappa_T^*)^{-1} = \rho^* \left(\frac{\partial P^*}{\partial \rho^*} \right)_{T^*}, \quad (25)$$

$$\alpha^* = \kappa_T^* \left(\frac{\partial P^*}{\partial T^*} \right)_{\rho^*}, \quad (26)$$

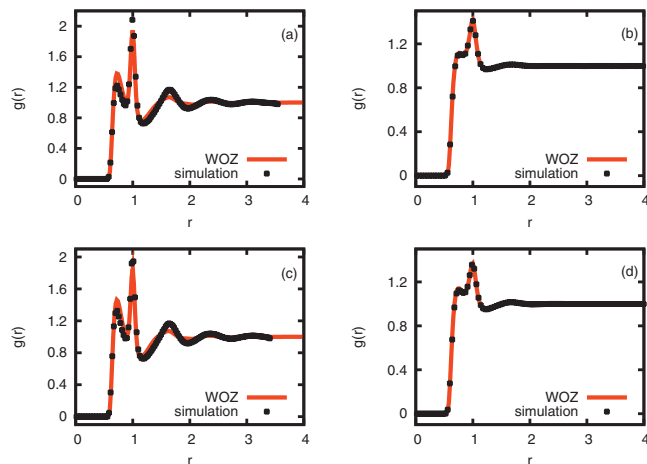


FIG. 2. Radial distribution function $g(r)$ at $P^* = 0.12$ for (a) $T^* = 0.15$ and (b) $T^* = 0.3$; $P^* = 0.19$ for panels (c) $T^* = 0.15$ and (d) $T^* = 0.3$.

$$C_p^* = C_v^* + \frac{\alpha^*}{\rho^*} \left[P^* - \rho^{*2} \left(\frac{\partial U^*}{\partial \rho^*} \right)_{T^*} \right]. \quad (27)$$

V. RESULTS AND DISCUSSION

Figure 2 shows the water radial distribution functions for two different temperatures and pressures, in reduced units. In general, the WOZ results are in good agreement with the MC results, although at lower temperatures, the integral equation

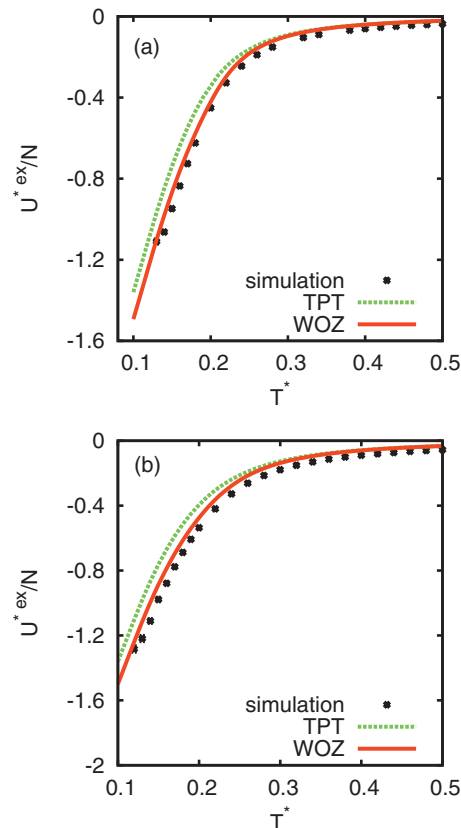


FIG. 3. Reduced excess internal energy per particle as a function of the reduced temperature. Panel (a) $P^* = 0.12$ and panel (b) $P^* = 0.19$. MC data are represented by symbols, TPT calculation by dashed, and WOZ by continuous line.

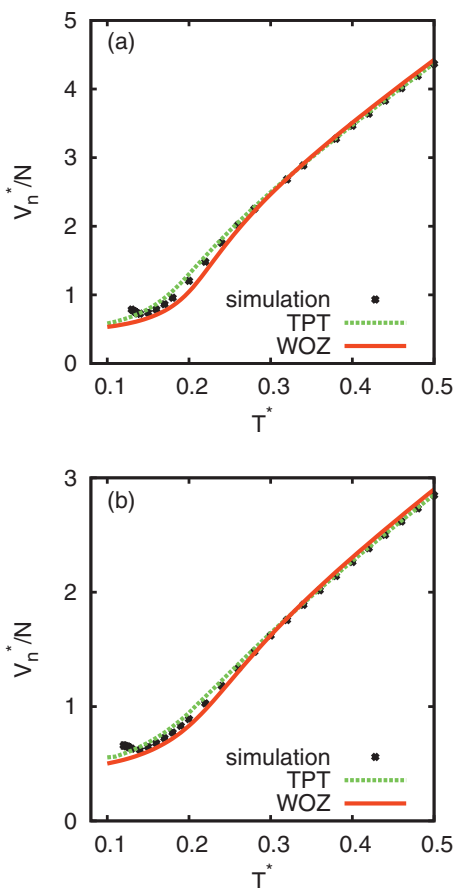


FIG. 4. Reduced molar volume per particle as a function of the reduced temperature for (a) $P^*=0.12$ and (b) $P^*=0.19$. Labeling as above.

theory slightly overestimates the LJ part of the interaction. The theory also predicts a second peak that is too low.

Figures 3–7 compare the energies, volumes, heat capacities, isothermal compressibilities, and thermal expansion coefficient versus temperature at two different pressures. All the state points presented on the graphs apply to the liquid phase. Figure 3 shows the reduced excess internal energy per particle as a function of the reduced temperature. Because of extensive hydrogen bonding of waters, the excess internal energy is more negative at lower reduced temperatures. At reduced temperatures below 0.2 the simulations were started from the crystal (cubic ice) structures and also from some previous liquid configuration using simulated annealing. If the crystal structure melted and the results (fluid density, pair distribution function) were found to be independent of the starting configuration, we take this as an indication of the liquid phase. In summary, for the range of temperatures where our water is in liquid form (above $T^* \approx 0.13$ for $P^* = 0.12$ and $T^* \approx 0.12$ for $P^* = 0.19$) the results of simulation do not depend on the starting configuration. Since thermodynamic perturbation and integral equation theories can only predict the liquid phase behavior, we focus on the liquid part of the phase diagram. As we see, both theories predict the excess internal energy quite well, especially at higher temperatures.

Figure 4 shows the reduced molar volume per particle as a function of the reduced temperature. The computer simulations successfully predict a minimum in the molar volume

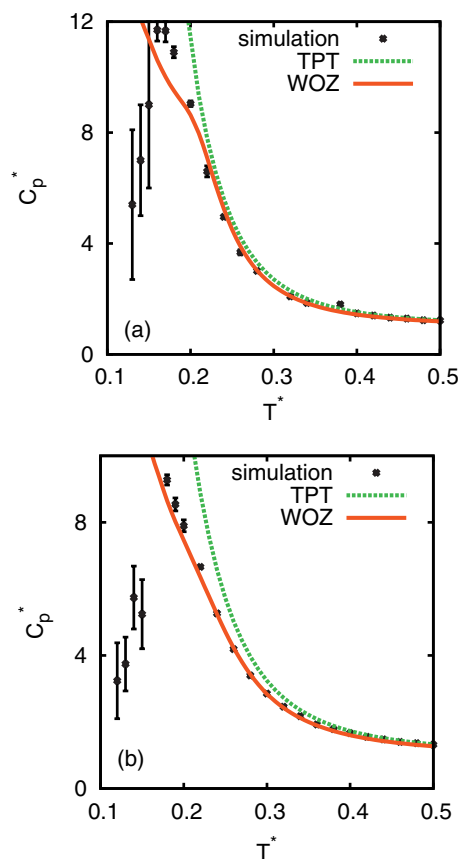


FIG. 5. Reduced heat capacity as a function of the reduced temperature: panel (a) $P^*=0.12$ and panel (b) $P^*=0.19$. Vertical bars indicate the uncertainties in MC simulations. Other labeling as above.

with temperature, as is found in real water. That is, if water is heated above its melting temperature, the molar volume first decreases, and after passing the minimum increases as normal liquids do. In contrast to the MC results, the analytical theories do not predict this minimum. However, at higher temperatures, both TPT and WOZ lead to good agreement with the computer simulations. An improved version of the TPT has been proposed recently.³² This approach, when applied to the 2D MB model, successfully predicted the minimum of the molar volume. That approach might succeed for the 3D model too.

Next we present the temperature dependence for other thermodynamic quantities of interest: (i) the reduced heat capacity, C_p^* , (ii) the reduced isothermal compressibility, κ_T^* , and (iii) the reduced thermal expansion coefficient, α^* . From the MC simulations, these quantities are calculated using the fluctuation formulas, hence, the uncertainties are considerably larger than for simpler averages such as the excess internal energy.

The reduced heat capacity, defined as $C_p^* = (\partial H^* / \partial T^*)_{P^*}$, reflects an extent to which HBs are broken upon heating. Breaking HBs is an “energy storage” mechanism of water that is not present in simple LJ fluids. Both theories (TPT and WOZ) predict well C_p^* at higher temperatures, but are much less successful at low temperatures. As expected, the predictions of the integral equation theory are superior to the TPT approach.

The compressibility curves shown in Fig. 6 are corre-

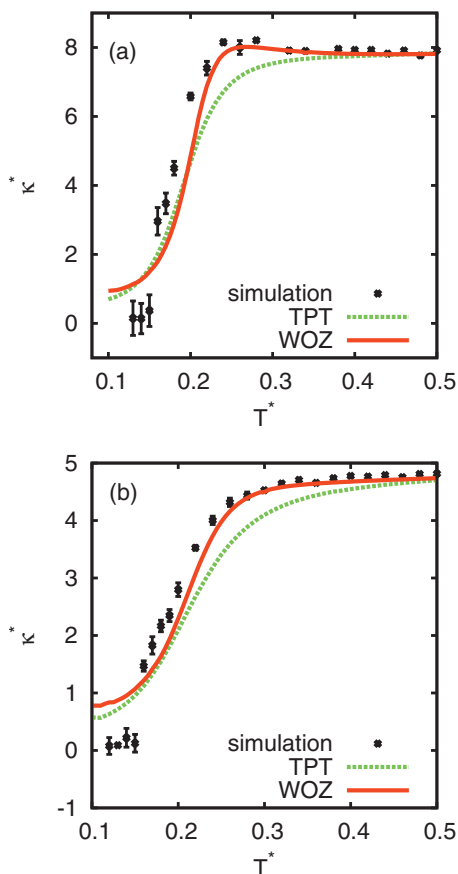


FIG. 6. Reduced isothermal compressibility as a function of the reduced temperature. Panel (a) $P^*=0.12$ and panel (b) $P^*=0.19$. Labeling as above.

lated with fluid density. As the density increases, the molecules get more closely packed and the fluid is more difficult to compress, so the compressibility decreases. The TPT and WOZ theories follow the MC results for this quantity quite well. As before, the integral equation theory yields better agreement with the machine simulations than the current version of the perturbation theory.

Figure 7 shows the reduced thermal expansion coefficient as a function of the temperature. Note that $\alpha^* = V^{*-1}(\partial V^*/\partial T^*)_{P^*}$ is merely a derivative of the function shown in Fig. 4. The model correctly predicts that the thermal expansion coefficient is negative at low temperatures, changing sign for the temperature where the molar volume of the model water has its minimum. Negative values of expansion coefficient are very small. The magnitude is the order of 10^{-1} . For very low temperatures fluctuations give unsatisfactory result. The main reason is in acceptance of trial moves, which was only around 1% because of a dense system. The TPT is in qualitative agreement with simulations, while the WOZ integral equation follows the simulation results quite well.

VI. CONCLUSIONS

Here, we study the 3D MB model of water. As our reference, we use (N, p, T) MC simulations. We compare against those simulations the results of two analytical theories, the TPT and WOZ integral equation theory. In the theories, the most substantial approximation is that the hydrogen

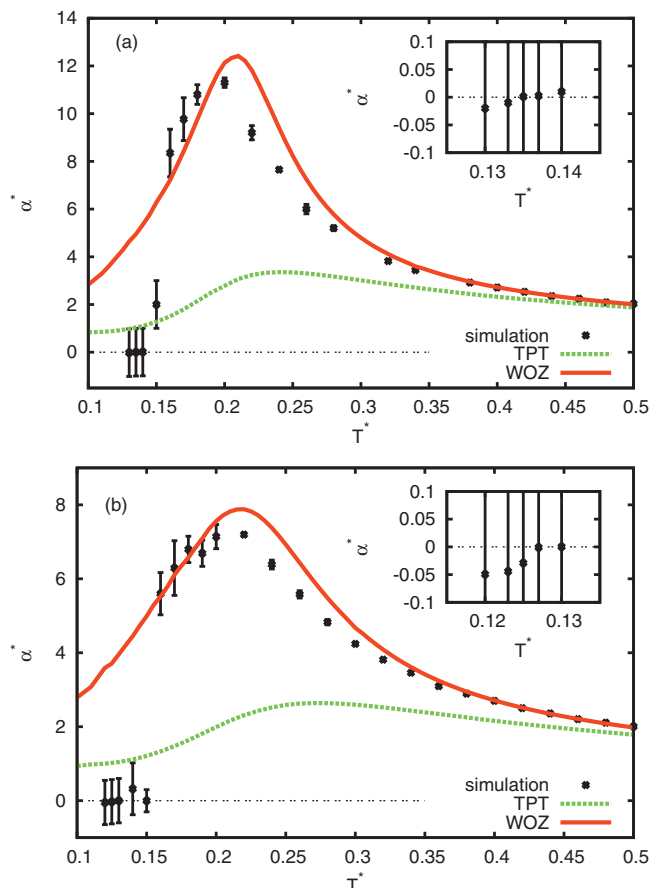


FIG. 7. Reduced thermal expansion coefficient as a function of the reduced temperature. Panel (a) $P^*=0.12$ and panel (b) $P^*=0.19$. Labeling as above.

bonding arms orient freely with respect to each other in a water molecule. Both analytical treatments are orders of magnitude more efficient than the computer simulations. For one state point at fixed temperature and pressure, computer simulation runs about 10^4 times longer than needed for the TPT or WOZ calculations. This means that these methods can be efficiently generalized to study solutions, and even mixtures with several solutes. The integral equation approach provides more accurate results than the TPT. We find that the analytical predictions are substantially better for hot water (high temperatures) than for cold water.

The principal challenge in modeling the physics of water comes from the orientation-dependent hydrogen bonding interactions. The integral equation theory used here is based on the orientationally averaged version of the OZ equation in the PPY closure.^{28,36,37} The theory in its present form is not able to predict the minimum in the molar volume found in the simulations. We think that this deficiency is due to the orientational averaging, which means that the intramolecular angle between the arms can assume a random value. There are two obvious directions for improvement: (i) to solve the orientation-dependent OZ equation³⁰ and/or (ii) to improve the PPY closure taking into account the ringlike structures. Notice that an orientational averaging is built in also in the TPT, where the reference system has a spherical symmetry. However, it has been previously shown for 2D MB water that both TPT and WOZ can be improved: the former by

using the local densities in calculation³² and the latter by a more sophisticated treatment of the orientational correlations³⁰ among the hydrogen bonding arms. We believe those steps may ultimately also be valuable for the 3D model and shall be considered next. As a result, a somewhat better agreement between theories and machine simulations is expected in the domain of low temperatures.

One key conclusion here is that the 3D MB model of water has many similarities with real water, including the volumetric and thermal anomalies. Our second main conclusion is that these analytical theories give good approximations to the properties of hot water, but they could benefit from better treatment of the orientational correlations for cold water. Another interesting conclusion of this study is that the 2D MB and 3D MB models of water provide similar insights. Based on previous results in 2D MB water, we also believe that this 3D MB model should be useful for studying the aqueous solvation of solutes. Current version of model does not correctly predict pair distribution function and cannot be used to study electrostatics and dielectric properties.

ACKNOWLEDGMENTS

This work was supported by the Slovenian Research Agency (Grant No. P1 0103-0201) and by the NIH (Grant No. GM063592).

¹D. Eisenberg and W. Kauzmann, *The Structure and Properties of Water* (Oxford University Press, Oxford, 1969).

²*Water, a Comprehensive Treatise*, edited by F. Franks (Plenum, New York), Vol. 1-7, pp. 1972-1980.

³F. H. Stillinger, *Science* **209**, 451 (1980).

⁴W. L. Jorgensen and J. Tirado-Rives, *Proc. Natl. Acad. Sci. U.S.A.* **102**, 6665 (2005).

⁵O. Markovitch and N. Agmon, *Mol. Phys.* **106**, 485 (2008).

⁶C. Tanford, *The Hydrophobic Effect: Formation of Micelles and Biological Membranes*, 2nd ed. (Wiley, New York, 1980).

⁷W. Blokzijl and J. B. F. N. Engberts, *Angew. Chem., Int. Ed. Engl.* **32**, 1545 (1993).

⁸G. Robinson, S.-B. Zhu, S. Singh, and M. Evans, *Water in Biology, Chemistry and Physics: Experimental Overviews and Computational Methodologies* (World Scientific, Singapore, 1996).

⁹K. A. Dill, T. Truskett, V. Vlachy, and B. Hribar-Lee, *Annu. Rev. Biophys. Biomol. Struct.* **34**, 173 (2005).

¹⁰P. Jungwirth and D. Tobias, *Chem. Rev.* **106**, 1259 (2006).

¹¹B. Hess, C. Holm, and N. van de Vegt, *Phys. Rev. Lett.* **96**, 147801 (2006).

¹²W. L. Jorgensen, J. Chandrasekhar, R. W. Madura, J. D. Impey, and M. L. Klein, *J. Chem. Phys.* **79**, 926 (1983).

¹³H. W. Horn, W. C. Swope, J. W. Pitera, J. D. Madura, T. J. Dick, G. L. Hura, and T. Head-Gordon, *J. Chem. Phys.* **120**, 9665 (2004).

¹⁴S. W. Rick, *J. Chem. Phys.* **120**, 6085 (2004).

¹⁵H. J. C. Berendsen, J. R. Grigera, and T. P. Straatsma, *J. Phys. Chem.* **91**, 6269 (1987).

¹⁶H. S. Ashbaugh, T. M. Truskett, and P. G. Debenedetti, *J. Chem. Phys.* **116**, 2907 (2002).

¹⁷P. H. Poole, F. Sciortino, T. Grande, H. E. Stanley, and C. A. Angell, *Phys. Rev. Lett.* **73**, 1632 (1994).

¹⁸I. Nezbeda, J. Kolafa, and Yu. V. Kalyuzhnyi, *Mol. Phys.* **68**, 143 (1989).

¹⁹I. Nezbeda, *J. Mol. Liq.* **73-74**, 317 (1997).

²⁰I. Nezbeda and G. A. Iglesias-Silva, *Mol. Phys.* **69**, 767 (1990).

²¹K. A. T. Silverstein, A. D. J. Haymet, and K. A. Dill, *J. Am. Chem. Soc.* **120**, 3166 (1998).

²²T. Urbic, V. Vlachy, Yu. V. Kalyuzhnyi, N. T. Southall, and K. A. Dill, *J. Chem. Phys.* **112**, 2843 (2000).

²³T. M. Truskett and K. A. Dill, *J. Phys. Chem. B* **106**, 11829 (2002).

²⁴B. Hribar, N. T. Southall, V. Vlachy, and K. A. Dill, *J. Am. Chem. Soc.* **124**, 12302 (2002).

²⁵A. Bizjak, T. Urbic, V. Vlachy, and K. A. Dill, *Acta Chim. Slov.* **54**, 532 (2007).

²⁶A. Ben-Naim, *J. Chem. Phys.* **54**, 3682 (1971).

²⁷A. Ben-Naim, *Water and Aqueous Solutions* (Plenum, New York, 1974).

²⁸M. S. Wertheim, *J. Stat. Phys.* **42**, 459 (1986).

²⁹M. S. Wertheim, *J. Chem. Phys.* **87**, 7323 (1987).

³⁰T. Urbic, V. Vlachy, Yu. V. Kalyuzhnyi, and K. A. Dill, *J. Chem. Phys.* **118**, 5516 (2003).

³¹T. Urbic, V. Vlachy, and K. A. Dill, *J. Mol. Liq.* **112**, 71 (2004).

³²T. Urbic, V. Vlachy, Yu. V. Kalyuzhnyi, and K. A. Dill, *J. Chem. Phys.* **127**, 174511 (2007).

³³T. Urbic and V. Vlachy, *Acta Chim. Slov.* **54**, 437 (2007).

³⁴C. L. Dias, T. Ala-Nissila, M. Grant, and M. Karttunen, *J. Chem. Phys.* **131**, 054505 (2009).

³⁵D. Frenkel and B. Smit, *Molecular Simulation: From Algorithms to Applications* (Academic, New York, 2000).

³⁶J. Chang and S. I. Sandler, *J. Chem. Phys.* **102**, 437 (1995).

³⁷E. V. Vakarin, Yu. Duda, and M. F. Holovko, *Mol. Phys.* **90**, 611 (1997).

³⁸J.-P. Hansen and I. R. McDonald, *Theory of Simple Liquids* (Academic, London, 1986).

³⁹N. F. Carnahan and K. E. Starling, *J. Chem. Phys.* **51**, 635 (1969).

⁴⁰D. J. Gonzalez, L. E. Gonzalez, and M. Silbert, *Mol. Phys.* **74**, 613 (1991).

⁴¹G. Jackson, W. G. Chapman, and K. E. Gubbins, *Mol. Phys.* **65**, 1 (1988).

⁴²M. S. Wertheim, *J. Chem. Phys.* **88**, 1145 (1988).

⁴³M. S. Wertheim, *J. Chem. Phys.* **85**, 2929 (1986).